HÖRZ, G. (1976). *Gase und Kohlenstoff in Metallen.* Edited by E. FROMM & E. GEBHART, pp. 84–201. Berlin: Springer-Verlag.
International Tables for X-ray Crystallography (1959). Vol. II, p. 300. Birmingham: Kynoch Press.
International Tables for X-ray Crystallography (1962). Vol. III, p. 235. Birmingham: Kynoch Press.
International Tables for X-ray Crystallography (1974). Vol. IV, p. 78, pp. 112–116, p. 149. Birmingham: Kynoch Press.
OHBA, S., SAITO, Y. & WAKOH, S. (1982). *Acta Cryst.* A**38**, 103–108.
OHBA, S., SATO, S. & SAITO, Y. (1981). *Acta Cryst.* A**37**, 697–701.
PHILLIPS, W. C. & WEISS, R. J. (1972). *Phys. Rev. B*, **6**, 4213–4219.
RAYNE, J. A. & CHANDRASEKHAR, B. S. (1961). *Phys. Rev.* **122**, 1714–1716.
SCHÄFER, H. (1964). *Chemical Transport Reactions* (translated by H. FRANKFORT), pp. 35–98. NY, London: Academic Press.
SHULL, C. G. & YAMADA, Y. (1962). *J. Phys. Soc. Jpn*, **17**, Suppl. B-III, 1–6.
STEVENS, E. D. (1974). *Acta Cryst.* A**30**, 184–189.
TORIUMI, K. & SAITO, Y. (1978). *Acta Cryst.* B**34**, 3149–3156.
WAKOH, S. & KUBO, Y. (1980). *J. Phys. F*, **10**, 2707–2715.
WAKOH, S. & YAMASHITA, J. (1971). *J. Phys. Soc. Jpn*, **30**, 422–427.
WEISS, R. J. & DEMARCO, J. J. (1965). *Phys. Rev.* **140**, A1223–1225.
WEISS, R. J. & MAZZONE, G. (1981). *J. Appl. Cryst.* **14**, 401–416.
ZACHARIASEN, W. H. (1967). *Acta Cryst.* **23**, 558–564.
ZACHARIASEN, W. H. (1968). *Acta Cryst.* A**24**, 421–424.

Acta Cryst. (1982). A**38**, 729–733

Anharmonic Thermal Vibrations and Atomic Potentials in Lead Fluoride (β-PbF_2) as a Function of Temperature

BY HEINZ SCHULZ, E. PERENTHALER AND U. H. ZUCKER

Max-Planck-Institut für Festkörperforschung, Heisenbergstrasse 1, *D*-7 *Stuttgart* 80, *Federal Republic of Germany*

(*Received* 1 *April* 1981; *accepted* 12 *May* 1982)

Abstract

Bragg intensities of β-PbF_2 (with the cubic fluorite structure) have been measured in the step-scan mode up to $\sin\theta/\lambda = 1{\cdot}17$ Å^{-1} at 295, 461 and 625 K by X-ray diffraction: $a = 5{\cdot}925\,(2)$, $5{\cdot}952\,(2)$, $5{\cdot}982\,(4)$ Å, respectively; $R = 0{\cdot}013$ for 103 reflections, 0·015 for 103 reflections, 0·018 for 106 reflections, respectively. The intensities were used for the refinement of anharmonic temperature factors up to third order for F^- and up to sixth order for Pb^{2+}. The temperature-factor formalism was based on the Gram–Charlier expansion. The probability density function (p.d.f.) of the F^- and Pb^{2+} ions were calculated from the coefficients of the anharmonic temperature factors. The p.d.f. maps gave clear evidence that the Pb^{2+} ions do not carry out isotropic thermal motion. The atomic potentials of the Pb^{2+} ions (derived from the p.d.f. maps) indicate that the thermal motion of the excited Pb^{2+} ions is strongly influenced by the repulsion terms along the Pb^{2+}–F^- bonds. The F^- ions carry out their largest thermal vibrations along $\langle 111 \rangle$ towards the centre of the elementary cell.

Introduction

β-PbF_2 crystallizes in the fluorite structure type. It exhibits a high F^- conductivity at medium temperatures. Furthermore, the F^- ions show pronounced anharmonic thermal vibrations along the body diagonals. Similar observations have been made for several other fluorides. The anharmonic part of the thermal motion of the F^- ions have been partly described by so-called split atoms or by a third-order temperature coefficient. Anharmonic thermal vibrations and ionic conductivity are closely related to each other. A discussion of these effects and a literature survey are given by Koto, Schulz & Huggins (1981). Only harmonic temperature factors have been applied to the lead ions in all of these investigations. Owing to the high point symmetry of the Pb^{2+} atomic position only an isotropic temperature factor is allowed for the harmonic model. If anharmonic thermal vibrations are considered, temperature factors (temperature tensors) of order four and six are allowed. The coefficients of these tensors can be determined by least-squares refinements of Bragg intensities. A discussion of the

0567-7394/82/050729-05$01.00

most frequently used formalisms of treating anharmonic thermal vibrations in crystals has recently been given by Zucker & Schulz (1982).

We have studied the anharmonic thermal vibrations of Pb^{2+} in β-PbF_2 as a function of temperature. The refinements have been extended up to temperature factors of the sixth order (tensors of rank six). Furthermore, we have used the refined coefficients to calculate the corresponding probability density functions. The effective atomic potentials were then derived from these p.d.f. maps.

Experimental

A crystal sphere with a diameter of 400 μm was ground from a larger piece of β-PbF_2 single crystal. This crystal sphere was put into a Lindemann-glass tube and fixed in its position by a second glass tube. Then both tubes were sealed by melting the tubes together. Their total length was approximately 2 mm. They were sealed in a quartz tube of about 10 mm length, which was put on a usual goniometer head. This arrangement was heated by a stream of hot air with an accuracy of ±3 K. Data collections were carried out at 295, 461 and 625 K.

Intensities were collected on a Philips automatic four-circle diffractometer in a step-scan mode with a step width of 0·045° and 60 steps, a scan velocity of 1·2° min^{-1}. ω ($\theta \leq 23°$) and $\omega/2\theta$ scans were applied. Data were measured up to $\sin\theta/\lambda = 1{\cdot}17$ $Å^{-1}$ for h unlimited and $k,l \leq 0$ for 295 and 461 K and h,k unlimited for 625 K. Ag $K\alpha$ radiation and a graphite monochromator were used.

The net intensities were calculated with the Lehmann–Larsen (1974) algorithm. The standard deviation of a single intensity measurement was calculated by $\sigma(I) = [\sigma'(I)^2 + (0{\cdot}01I)^2]^{1/2}$, with σ' the standard deviation calculated from the counting statistics and I the net intensity. The symmetry-equivalent reflections were averaged and corrected for absorption ($\mu r = 9{\cdot}5$). The final e.s.d.'s of the averaged and corrected intensities were calculated with the usual Gaussian error propagation law. The thermal diffuse scattering was corrected according to Skelton & Katz (1969) where the elastic constants of PbF_2 were taken from Simmons & Wang (1971). The complete data reduction was carried out with the program system *PROMETHEUS* (Zucker, Perenthaler, Kuhs, Bachmann & Schulz, 1982). Further details of the intensity measurements are listed in Table 1.

Table 1. *Details of data collection*

	295 K	461 K	625 K
Number of measured reflections	800	800	1567
Number of reflections with $I < 3\sigma(I)$	0	24	607
Number of symmetry-independent reflections	103	103	106
Number of symmetry-independent reflections with $I < 3\sigma(I)$	0	0	0
R value of symmetry-equivalent reflections (based on I)	0·053	0·059	0·12

Structure investigations

Scattering curves for Pb^{2+} and F^- and corrections for anomalous dispersion were taken from *International Tables for X-ray Crystallography* (1974). All structure calculations were carried out with *PROMETHEUS* (Zucker *et al.*, 1982). The structure investigation was focused on the thermal motion of the Pb^{2+} ions. The structure refinements were started with harmonic (isotropic) temperature factors for Pb^{2+} and F^-. Several extinction corrections were applied, but it turned out that extinction effects were not present. The refinements of the structure parameters were then expanded to anharmonic temperature factors based on the Gram–Charlier formalism [the reasons for using this formalism and details of the mathematical treatment are given by Zucker & Schulz (1982)]. Temperature factors up to sixth and third order were applied to Pb^{2+} and F^-, respectively.

The following refinement technique was applied. At first the order of the temperature factors was increased step by step. The coefficients of the temperature factors were then used to calculate the corresponding probability density functions of Pb^{2+} and F^- (*cf.* Zucker & Schulz, 1982). In this way the physical significance of the structure refinement was checked. The p.d.f. maps should show only positive values to be physically meaningful. This ideal situation can usually not be achieved owing to the limited amount and the limited accuracy of the measured intensities. Our experiences with PbF_2 and other substances show that, after the refinements with all temperature coefficients allowed by symmetry, the largest negative values of the p.d.f. maps are about 10% of the maximum probability density.

The next refinement step started with the selection of those temperature coefficients which are lower than their e.s.d.'s. The coefficient with the lowest absolute value was now taken as zero and it was kept zero during the next refinements. The newly refined coefficients were again used for the calculation of a p.d.f. map, which was compared with the first p.d.f. map. Further criteria were R values, goodness of fits and the change of e.s.d.'s. In this way we decided whether the first or the second refinement step gave the more reliable structure parameters. Now the next refinement step was started. This iterative procedure was repeated until a final convergence was reached. In this way the number of refined coefficients, their e.s.d.'s and their correlations could be reduced. Furthermore, the ratio of negative to positive probability densities could be considerably reduced to about 0·1%. The

Table 2. *Coefficients of the anharmonic temperature factors*

E.s.d.'s are given in parentheses. — allowed by symmetry, but not refined. The anharmonic temperature factor was used in the form

$$T = \exp(-B^{pq}h_ph_q)[1 + (2\pi i)^3/3!C^{pqr}h_ph_qh_r + (2\pi i)^4/4!D^{pqrs}h_ph_qh_rh_s + (2\pi i)^5/5!E^{pqrst}h_ph_qh_rh_sh_t + (2\pi i)^6/6!F^{pqrstu}h_ph_qh_rh_sh_th_u],$$

p,q,r,s,t,u = 1,2,3; repeating index summation assumed. Thermal parameters of the third, fourth and sixth order are multiplied by 10^3, 10^4 and 10^6, respectively. R and goodness-of-fit values are calculated with the observed reflections: $R1$ harmonic temperature factors, R (weighted); $R2$ harmonic temperature factors, R (unweighted); $R3$ anharmonic temperature factors, R (weighted); $R4$ anharmonic temperature factors, R (unweighted); GOF1 harmonic temperature factors; GOF2 anharmonic temperature factors.

	295 K	461 K	625 K
Pb^{2+}			
$B(11)$	0·0072 (1)	0·0107 (2)	0·0158 (4)
$B(22)$	0·0072 (1)	0·0107 (2)	0·0158 (4)
$B(33)$	0·0072 (1)	0·0107 (2)	0·0158 (4)
$D(1111)$	−0·00002 (1)	−0·0003 (2)	0·004 (1)
$D(2222)$	−0·00002 (1)	−0·0003 (2)	0·004 (1)
$D(3333)$	−0·00002 (1)	−0·0003 (2)	0·004 (1)
$D(1122)$	—	—	−0·0005 (4)
$D(1133)$	—	—	−0·0005 (4)
$D(2233)$	—	—	−0·0005 (4)
$F(111111)$	—	—	0·0018 (6)
$F(222222)$	—	—	0·0018 (6)
$F(333333)$	—	—	0·0018 (6)
$F(111122)$	−0·00005 (1)	−0·00007 (2)	−0·00016 (9)
$F(111133)$	−0·00005 (1)	−0·00007 (2)	−0·00016 (9)
$F(112222)$	−0·0005 (1)	−0·00007 (2)	−0·00016 (9)
$F(113333)$	−0·0005 (1)	−0·00007 (2)	−0·00016 (9)
$F(222233)$	−0·0005 (1)	−0·00007 (2)	−0·00016 (9)
$F(223333)$	−0·0005 (1)	−0·00007 (2)	−0·00016 (9)
$F(112233)$	—	—	−0·00014 (9)
F^-			
$B(11)$	0·0135 (5)	0·0206 (7)	0·023 (1)
$B(22)$			
$B(33)$			
$C(123)$	0·004 (2)	0·010 (4)	0·015 (6)
$R1$	0·018	0·017	0·017
$R2$	0·015	0·017	0·022
$R3$	0·016	0·016	0·015
$R4$	0·013	0·015	0·018
GOF1	3·7	2·8	3·0
GOF2	3·3	2·5	2·7

coefficients of the anharmonic temperature factors of PbF_2 refined in this way are listed in Table 2.*

Results and discussion

The decrease of the reliability factors (Table 2) and goodness-of-fit values when going from harmonic to

* Lists of structure factors for all three temperatures have been deposited with the British Library Lending Division as Supplementary Publication No. SUP 36918 (4 pp.). Copies may be obtained through The Executive Secretary, International Union of Crystallography, 5 Abbey Square, Chester CH1 2HU, England.

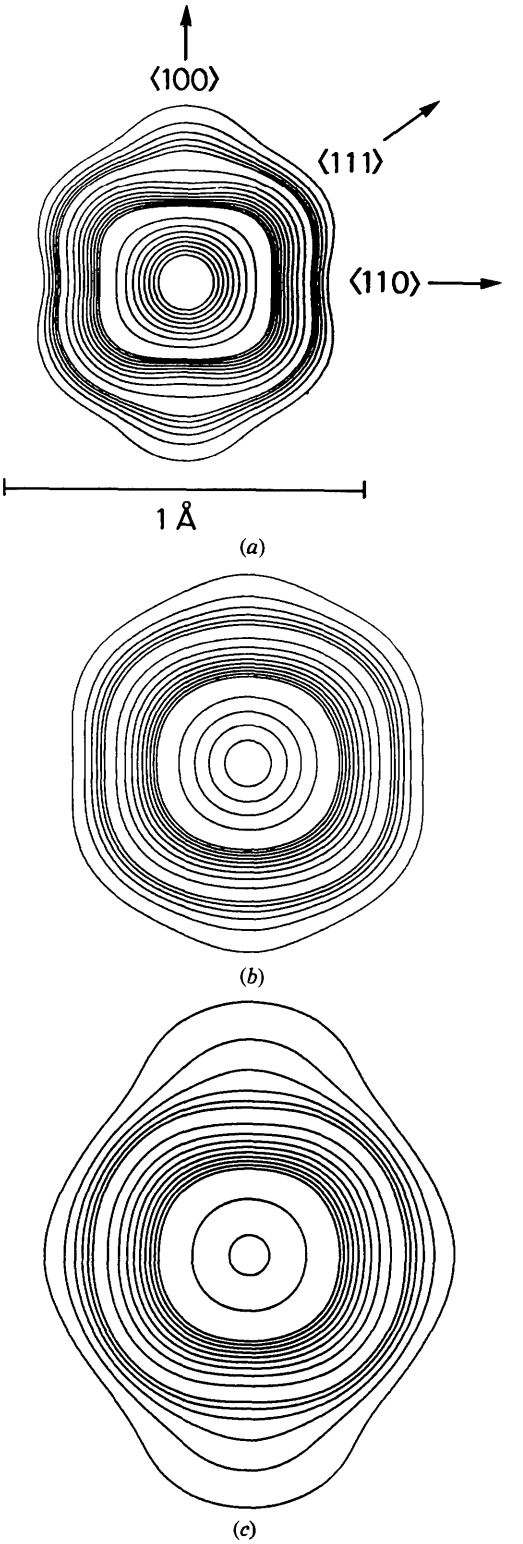

Fig. 1. Sections through the probability function of the Pb^{2+} ions. Lines are drawn from 0·1 to 1·0 $Å^{-1}$ in steps of 0·2 $Å^{-1}$, from 2 to 10 $Å^{-1}$ in steps of 1 $Å^{-1}$ and from 20 $Å^{-1}$ in steps of 10 $Å^{-1}$. Directions indicated in Fig. 1(*a*). Temperature: (*a*) 295 K; (*b*) 461 K; (*c*) 625 K.

anharmonic temperature factors point to the presence of anharmonic effects in PbF_2. [The change of the R values is significant as could be shown by Hamilton tests (Hamilton, 1965).] However, the direct interpretation of the coefficients of the temperature factors is rather hard, but they can be used to calculate the corresponding probability density maps (Zucker & Schulz, 1982).

Sections through the Pb^{2+} p.d.f. map are shown in Fig. 1. These sections reveal a clear trend with temperature. The p.d.f. maps become more flat and more extended with increasing temperature. They show the largest extension parallel to ⟨100⟩ at all three temperatures, if the outermost contour is considered. These are the directions to the second-nearest Pb^{2+} neighbours (Fig. 1). The direction of the smallest extension is, at room temperature, the ⟨100⟩ direction (first Pb^{2+} neighbour) and, at the highest temperature, the ⟨111⟩ direction (Pb^{2+}–F^- bond) (Fig. 1).

The p.d.f. maps can be used for the calculation of an effective one-particle potential (Zucker & Schulz, 1982). Fig. 2 shows potentials along the above-discussed main directions ⟨100⟩, ⟨110⟩ and ⟨111⟩. These potentials are derived from Fig. 1(*c*), the p.d.f. map of the highest temperature investigated, but they embody also the main features of the potential forms at lower temperatures.

Fig. 2 shows that the Pb–Pb potentials (⟨100⟩ and ⟨110⟩) become flat for the most excited Pb^{2+} ions in contrast to the Pb^{2+}–F^- potential (⟨111⟩) which does not show such a tendency. It follows that the thermal vibrations of the most excited Pb^{2+} ions are largest in the directions of the Pb neighbours and lowest in the directions of the F ions. Less excited ions behave in the opposite way.

This is just what one would expect from the structure of PbF_2. The less excited Pb^{2+} ions carry out small vibrations, which are hardly influenced by the repulsion terms. The repulsion can be considered as approximately linear with the shortening of a Pb^{2+}–F^- bond. Vibrations along ⟨111⟩ shorten only one Pb^{2+}–F^- bond (Δb). Vibrations along ⟨110⟩ shorten two Pb^{2+}–F^- bonds ($\Delta b'$) with $2\Delta b' > \Delta b$. Vibrations along ⟨100⟩ shorten four Pb^{2+}–F^- bonds ($\Delta b''$) with $4\Delta b'' > 2\Delta b'$. Therefore, we expect the steepest potential along ⟨100⟩ for less excited Pb^{2+} ions.

For the most excited ions the situation is just the opposite. The repulsion term now becomes very important along the Pb^{2+}–F^- bond. If we consider the same thermal vibrational amplitude, the shortest Pb^{2+}–F^- bond is generated for vibrations along ⟨111⟩, the medium bond length along ⟨110⟩ and the largest bonds for vibrations along ⟨100⟩. Therefore, the Pb^{2+} potential should become flattest along ⟨100⟩ with increasing excitation. This assumption is in agreement with our results (Fig. 2).

Only temperature factors up to third order could be refined for the F^- ions. The corresponding p.d.f. map and potentials are shown in Figs. 3 and 4. The p.d.f. map demonstrates clearly the preferred thermal vibrations of the F^- ions along ⟨111⟩ towards the centre of the elementary cell, which are the main directions for the F^- migration as already shown in an earlier investigation (Koto, Schulz & Huggins, 1981). The corresponding potential has the typical form of a pair

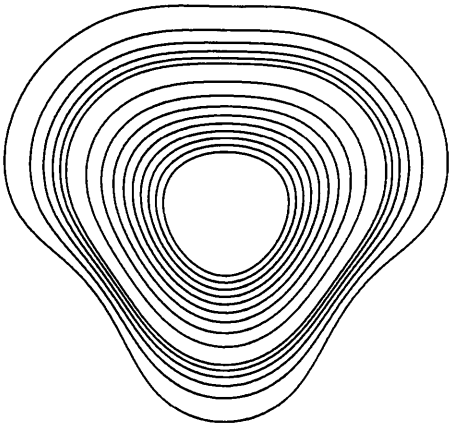

Fig. 3. Sections through the probability function of F^- ions at 625 K. Lines as in Fig. 1. Directions as indicated in Fig. 1(*a*).

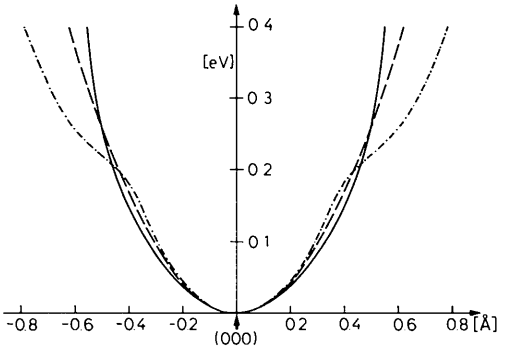

Fig. 2. Potential forms derived from Fig. 1(*c*). —— F^- bond direction ⟨111⟩; ---- next Pb^{2+} neighbour direction ⟨110⟩; —·— second Pb^{2+} neighbour direction ⟨100⟩.

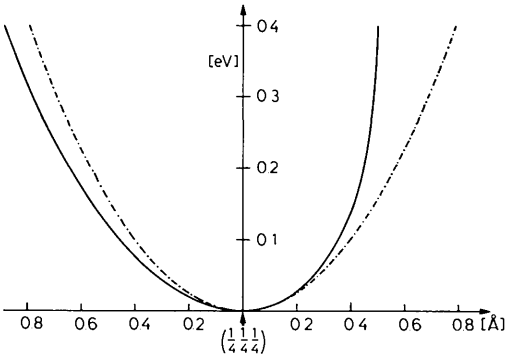

Fig. 4. Potential forms derived from Fig. 2: —— Pb^{2+} bond direction ⟨111⟩; —·— next F neighbour direction ⟨100⟩ and second F^- neighbour direction ⟨110⟩.

potential, steep towards the Pb^{2+} ions, flat towards the unoccupied center of the elementary cell. Our investigations do not show a difference in the potentials towards the nearest F^- neighbours ($\langle 110 \rangle$ and $\langle 100 \rangle$ directions), but these potentials are clearly steeper than in the $\langle 111 \rangle$ directions towards the center of the elementary cell.

Our investigations demonstrate that elastic X-ray diffraction data allow refinements of anharmonic temperature factors up to sixth order for the Pb^{2+} ions. These temperature factors and the corresponding p.d.f. maps allow the determination of one-particle potentials, which can be used to study the thermal vibrations of the Pb^{2+} ions in arbitrary directions.

We are very indebted to Dr J. Schoonman for supplying us with crystals and to Mr B. Mühlmann for technical assistance.

References

HAMILTON, W. C. (1965). *Acta Cryst.* **18**, 502–510.
International Tables for X-ray Crystallography (1974). Vol. IV. Birmingham: Kynoch Press.
KOTO, K., SCHULZ, H. & HUGGINS, R. A. (1981). *Solid State Ionics*, **1**, 355–365.
LEHMANN, M. S. & LARSEN, F. K. (1974). *Acta Cryst.* A**30**, 580–584.
SIMMONS, G. & WANG, H. (1971). *Single Crystal Elastic Constants and Calculated Aggregate Properties – A Handbook*. London: MIT Press.
SKELTON, F. E. & KATZ, J. L. (1969). *Acta Cryst.* A**25**, 319–329.
ZUCKER, U. H., PERENTHALER, E., KUHS, W. F., BACHMANN, R. & SCHULZ, H. (1982). *PROMETHEUS*. *J. Appl. Cryst.* Submitted.
ZUCKER, U. H. & SCHULZ, H. (1982). *Acta Cryst.* A**38**, 563–568.

Acta Cryst. (1982). A**38**, 733–739

Electric Field Gradients and Charge Density in Corundum, α-Al_2O_3

BY J. LEWIS AND D. SCHWARZENBACH

Institut de Cristallographie, Université de Lausanne, Bâtiment des Sciences Physiques, 1015 *Lausanne, Switzerland*

AND H. D. FLACK

Laboratoire de Cristallographie aux Rayons X, Université de Genève, 24, *Quai Ernest Ansermet,* 1211 *Genève* 4, *Switzerland*

(*Received* 28 *December* 1981; *accepted* 6 *May* 1982)

Abstract

The charge density in α-Al_2O_3 has been refined with respect to X-ray structure factors [complete spheres for both Mo $K\alpha$ and Ag $K\alpha$ radiations with $(\sin\theta/\lambda)_{max} = 1{\cdot}19$ and $1{\cdot}495$ Å^{-1} respectively] and electric-field-gradient tensors at both atomic sites, using Hirshfeld-type deformation functions. Atomic charges from a κ refinement are $+1{\cdot}32$ (5) for Al and $-0{\cdot}88$ (8) e for O. The charge distribution of O is polarized towards the four Al neighbours, and metal–metal bonds are clearly absent. Quadrupole coupling constants and asymmetry parameters of the field-gradient tensors cannot be determined from the structure factors. They define the quadrupolar deformations near the atomic centers, and the X-ray data define the charge density between the atoms. The orientational parameters of the tensors and the signs of their largest eigenvalues can be qualitatively retrieved from the X-ray data. The refinement of anisotropic secondary-extinction parameters may, however, destroy this information. Refinement with respect to the field gradients affects mainly the quadrupolar deformation terms, and has little influence on the X-ray scale factor (*i.e.* monopolar terms) and computed electrostatic fields (*i.e.* dipolar terms). Properties of the charge density with different angular symmetries are thus only weakly correlated.

Introduction

The structure of corundum, α-Al_2O_3 (Table 3), is usually described as a hexagonal close packing of O atoms, Al occupying two thirds of the octahedral interstices. The Al substructure is analogous to rhombohedral graphite. Each AlO_6 octahedron is thus linked with three other octahedra through common edges (honeycomb net) and with one octahedron

0567-7394/82/050733-07$01.00